### - Frontiers -

# COOPERATIVE FREE VOLUME RATE MODEL APPLIED TO THE PRESSURE-DEPENDENT SEGMENTAL DYNAMICS OF NATURAL RUBBER AND POLYUREA

RONALD P. WHITE, JANE E. G. LIPSON\*

DEPARTMENT OF CHEMISTRY, DARTMOUTH COLLEGE, HANOVER, NH 03755

RUBBER CHEMISTRY AND TECHNOLOGY, Vol. 92, No. 4, pp. 612–624 (2019)

## **ABSTRACT**

We apply the cooperative free volume (CFV) rate model for pressure-dependent dynamics of glass-forming liquids and polymer melts, focusing on two new applications of the model, to natural rubber and to polyurea. In CFV, segmental relaxation times,  $\tau$ , are analyzed as a function of temperature (T) and free volume ( $V_{\rm free}$ ), where the latter provides an insightful route to expressing dynamics relative to using the system's overall total volume (V).  $V_{\rm free}$  is defined as the difference between the total volume and the volume at close packing and is predicted independently of the dynamics for any temperature and pressure using the locally correlated lattice equation-of-state analysis of characteristic thermodynamic data. The new results for natural rubber and polyurea are discussed in the context of results on a set of polymeric and small-molecule glass formers that had previously been modeled with CFV. We also discuss the results in the context of recent connections that we have made with the density-scaling approach. [doi:10.5254/rct.19.80394]

### INTRODUCTION

In many applications of polymeric materials, it is important to understand their dynamic relaxation and how it is affected by temperature. Probing the influence of changing pressure on dynamics<sup>1,2</sup> can also be key and offers the opportunity for understanding, even under ambient conditions, how much of the change in relaxation time results purely from the change in *T* and how much from changing density. We (among others) have recently noted the analogy between pressure/density changes and confinement effects;<sup>3–7</sup> these are likely to play a role in situations in which interfaces are involved. In this article, we describe the application of our cooperative free volume (CFV) model<sup>7–11</sup> to understand and make predictions about segmental dynamics in a variety of materials, including two rubbery polymers of significant interest: polyurea (PU) and natural rubber (NR). We analyze experimental broadband dielectric relaxation (BDS) data on these systems and combine our new results with those from successful application of the CFV model to a range of other polymers as well as some small-molecule glass formers.

Numerous routes have been applied to the analysis of relaxation data on polymers in terms of thermodynamic variables. One widely known expression for connecting free volume with relaxation times was proposed by Doolittle. <sup>12</sup> In practice, because there was no independent route to free volume values, this relationship was used in historical models <sup>13–15</sup> to fit isobaric relaxation data and extract what turned out to be a temperature-dependent phenomenological function that was nominally termed the *free volume*. Although enjoying some degree of success, this approach was also viewed critically. In addition to the fit results providing no new insight, another problem was that this approach could not account for the effects of changing pressure, as shown by comparison of experimental P-dependent dynamics data with the corresponding volumetric data. <sup>1,2,10,16</sup> A more recent and will applied approach to analysis has involved the application of density-scaling methods. <sup>1,2,17–24</sup> Expressions in this category have been successfully used to analyze both temperature (T) and pressure (P) dependence of relaxation data. In density scaling, the general T, P-

<sup>\*</sup>Corresponding author. Email: jane.lipson@dartmouth.edu

dependent dynamics data are expressed such that relaxation times,  $\tau$ , are given by a function of the single combined variable,  $TV^{\gamma}$ , where  $\gamma$  is a material-specific parameter. The approach requires knowledge of the material's volume (V) and its temperature and pressure dependence (i.e., V[T,P]); full analysis of experimental relaxation data typically requires specifying four parameters to express the behavior functionally as  $\tau(T,V)$ . Values for the characteristic material-dependent parameter,  $\gamma$ , have been tabulated for a wide range of systems.

The CFV model<sup>7–11</sup> is a newer alternative. One difference between this and density-scaling treatments originates in our earlier work using a first-principles thermodynamic equation of state, the locally correlated lattice (LCL) theory,  $^{16,25}$  to predict relative free volumes in polymers and small-molecule glass formers. We noticed a strong linear correlation between the LCL prediction for a system's percent free volume at its glass transition ( $T_{\rm g}$ ) and the experimental value of that transition.  $^{16,26}$  This prompted our interest in whether the T- and P-dependent free volume ( $V_{\rm free}$ ) we predicted could be a useful metric for studying other points in the relaxation spectrum. In a following work,  $^{10}$  we then showed that, indeed,  $V_{\rm free}$  is a natural variable for analyzing and predicting dynamic relaxation data over a broad T and P range. Further, we were able to use our  $V_{\rm free}$  predictions along with experimental relaxation data to test the Doolittle relationship, show that it failed, and explain why.

As discussed in the following section, the CFV model is based on viewing local segmental relaxation as a rate process, having an activation energy that connects local cooperative motion to the availability of free volume sufficient to enable the local motion. The process is affected both by the availability of free volume and by temperature, which controls the thermal energy needed to overcome the activation barrier. The combined influence of free volume and temperature means that a change in experimental pressure, or the imposition of confinement effects through proximity to an interface, will be accounted for in the analysis and in making predictions. As will be discussed further below, one significant advantage of the CFV model is that it can be applied under conditions in which available dynamic data are sparse, since fewer material-specific parameters need be specified. Another advantage is that the CFV analysis is now leading us to model the effect of confinement on dynamic response, in particular how mobility and relaxation are changing as a function of position within nanometers of an interface. Finally, we have recently derived and demonstrated 11 a quantitative connection between the chief material-characteristic parameters of the CFV model and the density-scaling approach. This provides insight into both model frameworks and has the potential for significant expansion of CFV characterization to a very broad range of materials.

The remainder of this article is organized as follows. In the next section, we provide an overview of the LCL analysis, the CFV model, and the density-scaling model. Following this, in the "Results and Discussion" section, we present new results on PU and NR and discuss our findings in the context of our prior work on glassy materials. We also demonstrate the connection between CFV and density scaling. In the last section ("Summary"), we discuss some of the implications of our results and comment on future directions.

# THE CFV RATE MODEL AND DENSITY SCALING

The CFV rate model  $^{7-11}$  is a model for pressure-dependent dynamics describing segmental ( $\alpha$ ) relaxation times as a function of temperature and volume,  $\tau(T,V)$ . In CFV, the volume-based contribution to dynamics is expressed in terms of the system's thermodynamically characterized free volume,  $V_{\rm free}$ . The advantage in this is its efficiency, because the same single form (going as  $1/V_{\rm free}$ ) applies for all systems, and further,  $V_{\rm free}$  is determined without the need for dynamics data. We have found—and the CFV rate model predicts—that  $\ln \tau$  is a linear function of  $1/V_{\rm free}$  on isotherms, where each isotherm slope depends on the value of T.

 $V_{\rm free}$  is defined as the difference between a system's overall volume, V, and its limiting, closely packed, hard-core value,  $V_{\rm hc}$ .

$$V_{\text{free}} = V - V_{\text{hc}} \tag{1}$$

 $V_{\rm hc}$  is a constant for each system, independent of both T and P. It is determined via analysis of experimental PVT data using the LCL model equation of state (EOS), <sup>16,25</sup> detailed further below.

The physical meaning of the hard-core volume,  $V_{\rm hc}$ , is that it represents the limiting volume at close packing and quantifies the system's minimum possible volume. Although we use the LCL EOS in applications to experimental systems, we have made a strong connection with this close-packing interpretation in our simulation results on simple Lennard-Jones (LJ)-type systems. <sup>8,9</sup> The  $V_{\rm hc}$  value resulting from our simulation PVT data, which did not use LCL but extrapolated the PVT data down to zero T, was found to correspond closely to the volume of the LJ atoms at random close packing. When this  $V_{\rm hc}$  value was used to define  $V_{\rm free} = V - V_{\rm hc}$ , the corresponding plots of lnt versus  $1/V_{\rm free}$  isotherms were all linear.

In applications to experimental systems, the LCL EOS provides a convenient and unambiguous route to the prediction of  $V_{\rm hc}$ . As noted above, the LCL EOS is fit to the experimental system's PVT data, and  $V_{\rm hc}$  is thus obtained independent of any dynamics data. The LCL EOS P(V,T) expression for a compressible one-component system is given by

$$\frac{P}{k_{\rm B}T} = \left(\frac{1}{\nu}\right) \ln\left[\frac{V}{V - N_{\rm m}r\nu}\right] + \left(\frac{3}{\nu}\right) \ln\left[\frac{V - (N_{\rm m}\nu/3)(r-1)}{V}\right] \\
- \left(\frac{3}{\nu}\right) \left(\frac{(2r+1)^2}{(V/N_{\rm m}\nu) - (1/3)(r-1)}\right) \times \left(\frac{\exp[-\epsilon/k_{\rm B}T] - 1}{(1/3)(2r+1)\exp[-\epsilon/k_{\rm B}T] + (V/N_{\rm m}\nu) - r}\right) \tag{2}$$

where  $N_{\rm m}$  is the number of molecules and  $k_{\rm B}$  is the Boltzmann constant. The molecular parameters are r, the number of segments (occupied lattice sites) per molecule; v, the volume per lattice site; and  $\varepsilon$ , the segment–segment nonbonded interaction energy. The product of the molecular parameters, rv, describes the (constant) volume occupied per molecule, so  $V_{\rm hc}=N_{\rm m}rv$  is the limiting volume of the system at close packing (or in units of volume per gram,  $V_{\rm hc}=rv/M_{\rm w}$ , where  $M_{\rm w}$  is the molecular weight). Note when we evaluate  $V_{\rm free}(T,P)$ , we use the V(T,P) value from the LCL EOS (i.e., solving Eq. 2 at that T,P). The actual experimental V value (if available) would give essentially the same  $V_{\rm free}$  value if the chosen T,P point is inside the PVT data-fitting range (as the theoretical and experimental V's are very close). Extending outside the fitting range, we have found it better to stay consistently within the theory (i.e., using the theoretical V together with the theoretical  $V_{\rm hc}=N_{\rm m}rv$ ), as any errors will compensate/cancel. References 16 and 25 provide more background on the LCL model, and some further details related to the implementation of the LCL EOS for CFV are provided in ref 7 and in the appendix of ref 11.

The CFV rate model assumes segmental relaxation proceeds via a cooperative process in which the total activation free energy,  $\Delta A_{\rm act}$ , changes with the number,  $n^*$ , of cooperating particles (segments); an analogy can be drawn to the well-known treatment of Adam and Gibbs, <sup>27</sup> a model based on entropic considerations.

For a segment to break out of the cage of its surrounding neighbors and move, a characteristic amount of free space  $(v^*)$  is needed. The total number of nearby segments required to cooperate and open up this space is  $n^* = v^*/(V_{\text{free}}/N)$ , where  $V_{\text{free}}/N$  is the average free volume per particle at the given T,P condition. Each cooperating segment pays an energetic cost,  $\Delta a$ , and this adds up to give the overall total activation energy,  $\Delta A_{\text{act}} = n^* \Delta a$ .

The rate ( $\propto 1/\tau$ ) at which a segment enters a new opening is proportional to the rate it traverses a distance on the order of its own size ( $\propto$  velocity  $\propto T^{1/2}$ ), multiplied by the probability that a free space is available, given by the Boltzmann factor,  $\exp[-\Delta A_{\rm act}/T]$ . The general result is

$$1/\tau = \text{rate} = [\text{constant}] \times T^{1/2} \times \exp\left[-n^* \times \left(\frac{\Delta a(T)}{T}\right)\right]$$
$$= [\text{constant}] \times T^{1/2} \times \exp\left[-\left(\frac{1}{V_{\text{free}}}\right) \times f(T)\right]$$
(3)

The activation free energy per cooperating segment,  $\Delta a(T)$ , is some unknown function of temperature but not of volume. In our simulation results of the high T regime, a constant value of  $\Delta a$  is actually sufficient in Eq. 3, leading to an especially clear demonstration of how the total  $\Delta A_{\rm act}$  depends on volume and how the volume change (occurring at constant pressure) is an important source of non-Arrhenius behavior. Note that we have found the gas kinetic  $T^{1/2}$  contribution to be important in the high T regime. <sup>8,9</sup> At lower T in glassy systems, activation energies become high enough that the gas kinetic term can be dropped for simplicity, which is what we do in the model applications addressed here.

Equation 3 then leads to the following working form of the CFV equation, which is applicable for modeling structural/segmental dynamics of experimental liquids probed via dielectric spectroscopy.

$$\ln \tau = \left(\frac{V_{\text{hc}}}{V_{\text{free}}}\right) \left(\frac{T^*}{T}\right)^b + \ln \tau_{\text{ref}} \tag{4}$$

where  $b, T^*, \tau_{\rm ref}$ , are material-specific parameters. Here we use the relative free volume,  $V_{\rm free}/V_{\rm hc}$  (e.g., rather than  $V_{\rm free}/N$ ) because it is convenient. The form of the T dependence,  $\Delta a(T)/T = f(T) \sim 1/T^b$ , is empirical, but it has been found to work very well. We apply Eq. 4 to a variety of experimental systems below.

Another important model in the study of pressure-dependent dynamics is the density-scaling approach. In a recent article we compared this approach with CFV and also demonstrated some strong connections between the two methods. The density-scaling approach can be described as the expectation that general P-dependent dynamics data can be expressed (collapsed) such that relaxation times are given by  $\tau = F(TV^T)$ , with  $\tau$  being a function of the single combined variable,  $TV^T$ , where  $\gamma$  is a material-specific parameter and T is some function of unspecified form.

A way to appreciate the source of the power law form of density scaling is to consider connections with the behavior of the simple, purely repulsive, inverse power law fluid, which has a pair potential going as  $u(r) \propto 1/r^n$  and dynamic properties that depend only on  $TV^{n/3}$ ,  $^{28}$ ,  $^{29}$  which thus implies  $n/3 = \gamma$ . This simple system provides the opportunity to connect thermodynamic and dynamic properties. Further insight into why density scaling works is available in the context of the isomorph theory of Dyre and coworkers  $^{19}$ ,  $^{20}$  and a body of related simulation works that have connected dynamics with some of the thermodynamic properties that are available from simulation. Examples include the simulation works of Pedersen et al.  $^{30}$ ,  $^{31}$  and Coslovich and Roland  $^{32-34}$  showing that the averaged slope of the correlations between the virial and the energy can lead to the value of the system's  $\gamma$  parameter.

In addition to simulated model fluids, density scaling with the  $\gamma$  parameter has been widely applied in the analysis of P-dependent dynamics data for real experimental systems, which is the focus of this article. Here, because of the lack of detailed thermodynamic information of the sort described above, the value for  $\gamma$  must typically be determined by fitting experimental dynamics data. Real experimental systems have commonly been modeled using the analytic  $\tau(T,V)$  expression developed by Casalini et al.,  $^{22,23}$  in which the T,V density-scaling form was derived

using the Avramov entropy model,<sup>35</sup> and this is given by

$$\ln \tau = \left(\frac{A}{TV^{\gamma}}\right)^{\phi} + \ln \tau_0 \tag{5}$$

Equation 5 includes the  $\gamma$  parameter, along with three other material-specific parameters,  $\phi$ , A, and  $\tau_0$ .

It turns out that there is a strong connection between the CFV b parameter and the  $\gamma$  parameter from the density-scaling approach, and we have recently how how they are analytically related. Making the connection between b and  $\gamma$  starts with the relationships that define each parameter; these are  $b = -(\partial \ln V_{\rm free}/\partial \ln T)_{\tau}$  and  $\gamma = -(\partial \ln T/\partial \ln V)_{\tau}$ , which are apparent from Eqs. 4 and 5, respectively. Both parameters serve to quantify a system's relative sensitivity to changes in temperature versus changes in (free) volume. For example, a large  $\gamma$  means that for a given (relative) change in volume, there would have to be a large (relative) change in T to compensate and keep  $\tau$  fixed, and thus systems with large  $\gamma$  are strongly volume sensitive, whereas those with small  $\gamma$  are more sensitive to temperature. By corresponding arguments, large b indicates strong temperature sensitivity, whereas small b indicates stronger sensitivity to (free) volume.

The relationship for  $\gamma$  can be written in terms of free volume as follows.

$$\gamma = -\left(\frac{\partial \ln T}{\partial \ln V}\right)_{\tau} = -\left(\frac{\partial \ln T}{\partial \ln V_{\text{free}}}\right)_{\tau} \frac{d \ln V_{\text{free}}}{d \ln V} = -\left(\frac{\partial \ln T}{\partial \ln V_{\text{free}}}\right)_{\tau} \frac{V}{V_{\text{free}}}$$
(6)

In Eq. 6,  $d\ln V_{\rm free}/d\ln V = V/V_{\rm free}$  follows from the simple definition  $V_{\rm free} = V - V_{\rm hc}$  (Eq. 1), where  $dV_{\rm free}/dV = 1$ . Substituting  $b = -(\partial \ln V_{\rm free}/\partial \ln T)_{\tau}$  into Eq. 6, we obtain the relationship between  $\gamma$  and b.

$$\gamma = \frac{1}{b(V_{\text{free}}/V)} \approx \frac{1}{b(V_{\text{free}}/V)_{@T_{\sigma}}} \tag{7}$$

The relationship between  $\gamma$  and b technically carries a density dependence because of the presence of the multiplicative factor,  $V_{\rm free}/V$ , the fractional free volume. Over the operating range of the P-dependent analysis,  $V_{\rm free}/V$  may vary by about a factor of two. To convert between the two parameters, the key is to choose a single  $V_{\rm free}/V$  value that is representative of the average  $V_{\rm free}/V$  of this range. It is reasonable to expect that this should work because we know that a constant b and a constant  $\gamma$  each work well to describe data within their respective model frameworks. The  $V_{\rm free}/V$  value at the ambient  $T_{\rm g}$  is a good single choice. This is because being both at a low T and a low T results in an intermediate density, putting it roughly in the middle of the range of the  $V_{\rm free}/V$  values over a typical P-dependent data set. The  $V_{\rm free}/V$  value at the system ambient  $T_{\rm g}$  is denoted as  $(V_{\rm free}/V)_{\tiny (M_{\rm grg})}$ , and this gives the operating relationship connecting each system's  $\gamma$  and b,  $\gamma \approx 1/[b(V_{\rm free}/V)_{\tiny (M_{\rm grg})}]$ , which is the right-hand form in Eq. 7. This approximate expression is quite effective, and we will discuss the results covering a range of experimental systems below.

# RESULTS AND DISCUSSION

In this work, we tackle the CFV analysis of rubbery polymers for the first time, focusing on PU and NR. The experimental data for both systems reflect some degree of sample complexity. In the case of NR, the samples studied by Ortiz-Serna et al.<sup>36</sup> originate from the *Hevea brasiliensis* tree and also include some vulcanization additives. In analyzing their dielectric relaxation data, the authors were able to identify backbone segmental motion, which they assign as their  $\alpha$  peak, and probe the effect of changing both temperature and pressure on relaxation. They collected data on both wet and dry samples and showed that the  $\alpha$  process was unaffected by the difference in

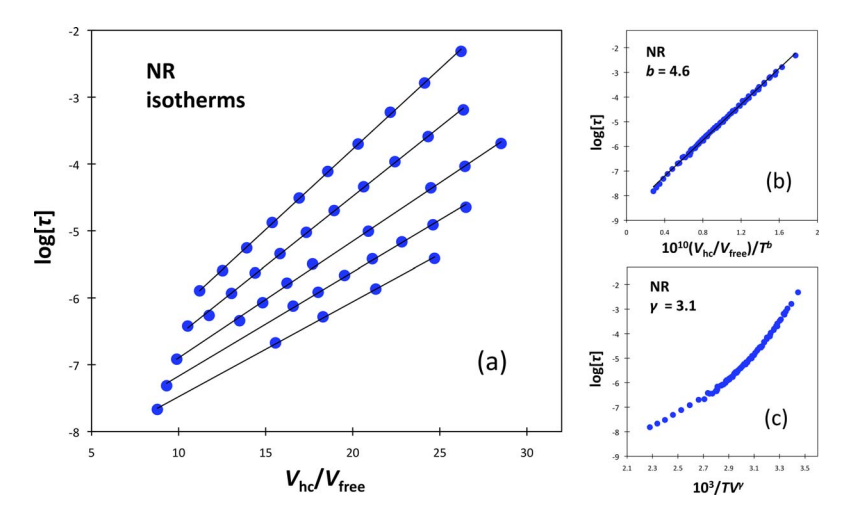


FIG. 1. —  $T_rP$ —dependent  $\alpha$ -relaxation times ( $\tau$ ) for natural rubber (NR). (a) log $\tau$  vs inverse relative free volume ( $V_{hc}/V_{free}$ ), plotted as isotherms. Symbols mark each experimental relaxation time at the corresponding  $V_{hc}/V_{free}$  value, calculated independently via LCL EOS analysis of the PVT data. References for experimental data are available in Table I. Isotherms correspond to T=268, 278, 288, 298, and 308K (lines are the corresponding linear fits); pressure values range from 1 atm up to 240 MPa. (b) and (c) show collapsed plots of the same  $T_rP$ —dependent data (and with the isotherms at 273, 283, 293, 303, and 313K also included). CFV model (b):  $\log \tau$  vs ( $V_{hc}/V_{free}$ )/ $T_r^b$ , where b=4.6 (T in K). Density scaling (c):  $\log \tau$  vs  $1/TV^r$ , where y=3.1 (T in K, V in mL/g).

conditions. In what follows, we present our analysis of data on the wet samples, which correspond to having the natural fraction of water content for samples exposed to ambient conditions, but note that similar results would accrue from studying the dried samples.

The PU analysis makes use of data reported by Roland and Casalini,  $^{37}$  and here it is useful to note that *polyurea* actually refers to a category of block copolymers, in which a "soft" diisocyanate block is polymerized with an oligomeric diamine. Varying the ratios of reactants will result in control over the fraction in the sample of the "softer" segments having lower  $T_{\rm g}$ , relative to the harder segments (associated with the cross-linking regions), which have significantly higher  $T_{\rm g}$ . The presence of these two different kinds of regions leads to a combined set of mechanisms for energy dissipation, and the ability to vary their ratio creates the opportunity for tuning structural and material properties. Another appealing feature of this group of polymers is that spray application methods have led to film formulations that cure rapidly over a wide range of humidity and temperature. The result is that PU has generated significant interest in its applications, including as a retrofit coating to protect against ballistic and shockwave impact. <sup>38</sup>

The sample studied in ref 37 was produced using a ratio of 1:4 isocynate to amine (and annealed to a water content of 3.5%). The dynamics of the soft segments were probed in a T range of 232 to 299K, with the dynamic  $T_{\rm g}$  at atmospheric pressure appearing to be around 225K (figure 3 of ref 37). The  $T_{\rm g}$  of the hard segments is much higher, estimated to be greater than 400K. Therefore, only the soft segments were taken to be contributing to the dynamic relaxation data. We note that the presence of both hard and soft regions in PU leaves some uncertainty in regard to how to analyze the free volume. The PVT analysis we undertook on PU assumes a homogeneous sample. Although it seems clear that the contributions from the soft segments should make a stronger contribution to how  $V_{\rm free}$  changes with T and P, here we take the simplest approach and do not attempt to assign a fraction of  $V_{\rm free}$  to the soft segments.

In Figure 1a, we show the series of isotherms arising from CFV analysis, in which log  $\tau$  is plotted against the inverse relative free volume.  $V_{hc}$  and  $V_{free}$  were predicted using the LCL theory

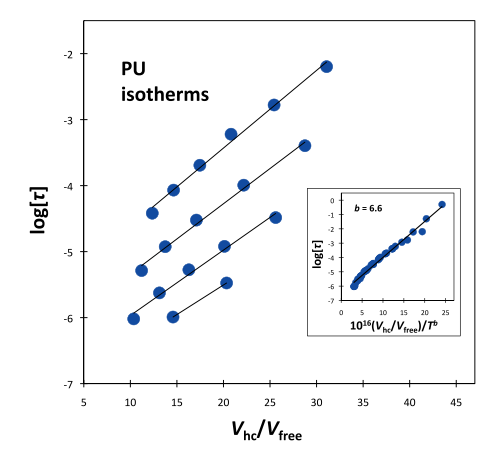


FIG. 2. —  $T_{,P}$ —dependent  $\alpha$ -relaxation times ( $\tau$ ) for polyurea (PU). Main plot:  $\log \tau$  vs inverse relative free volume ( $V_{ho}/V_{free}$ ), plotted as isotherms. Symbols mark each experimental relaxation time at the corresponding  $V_{ho}/V_{free}$  value, calculated independently via LCL EOS analysis of the PVT data. References for experimental data are available in Table I. Isotherms correspond to T=267.7, 283.8, 298.6, and 312.3 K (lines are the corresponding linear fits); pressure values range from 1 atm up to 260 MPa. Inset: collapsed plot of the same  $T_{,P}$ —dependent data (and with the data collected on the ambient pressure isobar also included); shows  $\log \tau$  vs ( $V_{ho}/V_{free}/T^b$ , where b=4.6 (T in K).

applied to (thermodynamic) PVT data. As we have found in all the materials studied so far, the LCL free volume emerges as a natural variable in the CFV model, a conclusion supported by the unambiguously linear set of isotherms, whose slopes increase as the temperature drops. In prior work<sup>7–9,11</sup> introducing the CFV expression, we have discussed why the form of the volume contribution goes as inverse free volume in particular and why the slopes are T dependent. Mechanistically, the general form embodies a model view of cooperativity that reflects the combined requirement of free volume along with thermal activation for each participating segment (see Eq. 3). The details of the temperature dependence of the isotherms is captured by using the full

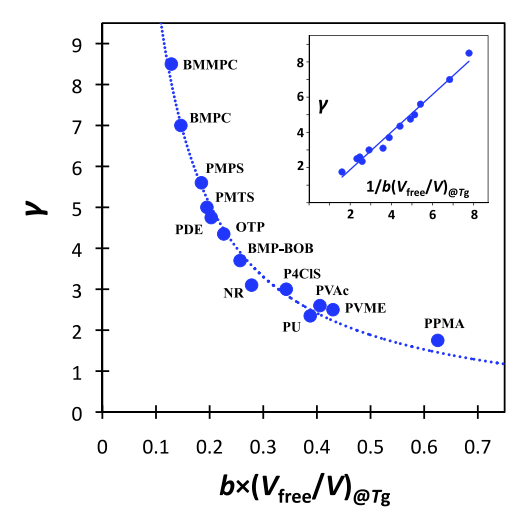


FIG. 3. — Relationship (Eq. 7) between the  $\gamma$  parameter and the CFV b parameter for polymers and small-molecule liquids:  $\gamma$  vs  $b(V_{\text{free}}/V)_{@T_g}$  (with smooth fit hyperbola). Inset:  $\gamma$  vs  $1/(b(V_{\text{free}}/V)_{@T_g})$  (with corresponding linear fit). System acronyms are marked in the figure. Acronym definitions and references for  $\gamma$  values and experimental data are available in Table I.

CFV expression (Eq. 4), which means plotting against  $(V_{\rm hc}/V_{\rm free})^*(1/T^b)$ , with b optimized by inspection. The result is a single straight-line plot, shown in the upper right (Figure 1b), where we obtain a value of b=4.6 and where values for the remaining two dynamics-related constants,  $\tau_{\rm ref}$  and  $T^*$ , may now simply be read off of the plot from its slope and intercept. ( $T^*=237$ K, and  $\log \tau_{\rm ref}=-8.66$ .) We emphasize that, having parameterized the LCL EOS data using thermodynamic data to predict the  $V_{\rm free}$  values, only one dynamics parameter (b) remains to be optimized to capture fully the experimental relaxation data across the entire T and P range.

In Figure 1c, we also show the collapse of the relaxation data according to the density-scaling approach. In that case, the abscissa is  $1/TV^{\gamma}$ ; temperature and volume also are key in this analysis; however, it is the total (not free) volume that is scaled, here using  $\gamma$ . The  $\gamma$  value for NR has not yet been made available in the literature. Here, we find that  $\gamma = 3.1$ . The curve shown in Figure 1c can be expressed using Eq. 5, and optimization leads to the values for its three additional dynamics parameters: A,  $\phi$ ,  $\tau_0$ . (We find A = 423 [mL/g] $^{-\gamma}K^{-1}$ ,  $\phi = 4.87$ ,  $\log \tau_0 = -8.56$ .) It is interesting to compare our  $\gamma$  value of NR with values reported for cis-1,4-polyisoprene, of which NR is principally composed. In Fragiadakis et al.,<sup>39</sup> values of  $\gamma = 3.4$  and 3.7 were found for two low-molecular-weight samples; these are reasonably close to the value found here for NR, but a little higher, which is sensible as  $\gamma$  generally increases with decreasing molecular weight.<sup>40–42</sup>

Figure 2 shows the analogous CFV analysis for the PU data. The T and P ranges covered for the PU analysis are similar to that for the NR data, spanning roughly 268 to 312K and ambient pressure up to about 260 MPa. The collapsed data set for PU, obtained using a value of b=6.6, is shown as an inset. The density-scaling result was reported in Roland and Casalini, <sup>37</sup> who obtained  $\gamma$ =2.35. We note that the ref 37 data extend to pressures greater than 260 MPa; the CFV model can still be applied to these data with fair agreement, although there is some downward curvature in the isotherms at these very high pressures. It is possible that the extension to higher P data could be improved by correcting the  $V_{\rm free}$  prediction so that it reflects only the soft segments, because only that portion of the sample contributes to the dielectric response.

As outlined in the previous section, the CFV b and the density-scaling  $\gamma$  parameters are directly related, and one may be obtained from the other if a representative  $V_{\rm free}/V$  value is chosen to connect the two (Eq. 7). For reasons described above, we use  $V_{\rm free}/V$  evaluated at the ambient glass transition of the material in question. Figure 3, in which we combine the points from the two new studies reported here with those from our recent prior work, 11 illustrates the correspondence between the two. The inset demonstrates that the linear relationship described by Eq. 7 indeed holds, supporting the assumption that choosing a constant representative value for the fractional free volume (in particular, the value at the ambient  $T_g$  for each sample) retains the robust connection derived in Eq. 6.

In Table I, we tabulate the full set of CFV dynamic and LCL thermodynamic parameters, as well as the  $\gamma$  values and data references, for all the systems we have studied to date. In some cases, the  $\gamma$  values derive from our own implementation of density-scaling analysis, whereas most come directly from the literature (e.g., many have been tabulated in the Roland et al. review). We recently demonstrated that the smaller number of model parameters required to fit the dynamics data in the CFV model (b,  $T^*$ ,  $\tau_{ref}$  as opposed to  $\gamma$ ,  $\phi$ , A,  $\tau_0$  in Eq. 5) results in our ability even under very sparse data conditions to characterize fully the dynamic response. Given a full set of thermodynamic data (e.g., PVT results, along with  $T_g$  values for at least two pressures), we can fully implement the CFV model using as few as two ambient-pressure relaxation data points and then predict the dynamic response at other pressures. We have shown, for example, that such predictions are in excellent agreement with experimental results on poly(vinylacetate). This flexibility means that we can use the CFV model under conditions in which the data are insufficient to apply the Eq. 5 density-scaling expression or insufficient even to obtain the  $\gamma$  parameter alone. In the latter case, see the example in ref 11, in which by implementation of Eq. 7, we could still use CFV to predict the correct  $\gamma$  value.

 ${\bf TABLE\ I}$  System Dynamics^a and EOS^b Parameters and Experimental References

			О	CFV parameters	eters		LCL EOS characterization	racterization		References	seou
System <sup>c</sup>	$T_{ m g},{ m K}$	λ	q	$T^*$ , K	$\log \tau_{\mathrm{ref}}$ , s	$V_{ m hc}$ , mL/g	r/M <sub>w</sub> , mol/g	$\nu$ , mL/mol	–ε, J/mol	$\tau(T,P)$ data	PVT data
$PVAc^d$	305	2.6	3.90	421	-10.2	0.7583	0.1379	5.499	1805	43, 44	45
PVME	242	2.5		272	-8.28	0.8665	0.1306	6.635	1782	46	47
<b>PMPS</b>	246	5.6		356	-16.4	0.8138	0.1147	7.095	1901	48	49
PMTS	261	5.0		465	-16.5	0.7177	0.1078	6.658	1717	50	49
PPMA	323	1.75		351	-6.25	0.8505	0.09904	8.587	1988	51	45
$P4CIS^e$	391	3.0		634	-12.3	0.7401	0.09678	7.647	2187	52	45
NR	220	3.1		237	-8.66	0.9982	0.1378	7.245	1843	36	45
PU	225	2.35		228	-6.44	0.8209	0.1341	6.124	1929	37	37
BMPC	241	7.0		536	-17.7	0.8179	0.2242	3.648	1677	53	54
<b>BMMPC</b>	261	8.5		268	-15.4	0.8338	0.1961	4.252	1858	55	54
PDE	295	4.75		548	-14.9	0.6587	0.1293	5.095	1906	56	57
OTP	244	4.35		380	-14.7	0.8202	0.1410	5.817	1720	58	59
BMP-BOB	231	3.7		266	-10.6	0.7105	0.1655	4.293	1807	09	61

ollowed by a linear fit for T\* and Tref gives similar results. y is a system-dependent parameter for the density scaling approach. Most of the y values come from table 2 of Roland et al. For the emaining values,  $\gamma$  for polyurea is from ref 37 and that for BMP-BOB is from ref 61;  $\gamma$  values for NR and PPMA were obtained by us, by collapsing the log  $\tau$  vs 1/TV' data, and also for OTP b The LCL EOS molecular parameters are as follows: r, number of segments (occupied lattice sites) per molecule; v, volume per lattice site; and e, segment-segment nonbonded interaction  $^a$  b,  $T^*$ , and  $\tau_{\rm ref}$  are system-dependent parameters for the CFV model, most were obtained by simultaneous 3-parameter fitting of the  $\tau(T,P)$  data to Eq. 4. As noted, first collapsing data for b, energy.  $M_{\infty}$  is the molecular weight. The hard-core volume,  $V_{\text{hc}}$ , per molecule, is obtained from the product rv, and  $V_{\text{free}}$  is defined as  $V-V_{\text{hc}}$ . See the appendix in ref. 11 for more information on because  $\gamma = 4.35$  gives a somewhat better collapse of the dielectric data<sup>38</sup> than the commonly reported  $\gamma = 4.00$ . The  $\gamma$  for P4CIS is via PVT-based  $T_e(P)^{7.45}$  and equation 38 of ref 1. LCL EOS implementation.

<sup>c</sup> System acronyms and info: PVAc, polyvinylacetate; PVME, polyvinylmethylether; PMPS, poly methylphenylsiloxane; PMTS, poly methyltolylsiloxane; PPMA, polypropylmethacrylate; NR, natural rubber; PU, polyurea; BMPC, 1,1'-bis(p-methoxyphenyl)cyclohexane; BMMPC, 1,1'-di(4-methoxy-5-methylphenyl)cyclohexane; PDE, phenolphthalein-dimethyl-ether; OTP, orthoterphenyl; BMP-BOB, 1-butyl-1-methylpyrrolidinium bis[oxalate]borate. Typically for most systems, the dynamic data points we modeled cover pressure ranges from P=1 atm (0.1 MPa) to about 200 MPa and in some cases up to 400 or 500 MPa. Temperature values varied with the system and are available in the experimental references.

d PVAc has been used as an example system to test different parameterization routes and data availability scenarios, so we have discussed several slightly different parameters sets. The set isted in this table  $(b \approx 3.9)$  is from fitting to a very large P-dependent dynamics data set including pressures all the way up to 400 MPa. Other fits of b have been centered on somewhat lower pressures (e.g., 0 to 200 MPa), and so b was closer to  $\approx 3.6$  to 3.7. All of these values are effectively close, and in general, we observe that anywhere in this range of b gives very good data collapse in plots of  $\ln \tau$  vs  $V_{hc}/(V_{\text{free}}T^b)$ .

<sup>e</sup> Only ambient pressure dynamics data were available for P4ClS, so it was characterized using these data combined with information on  $T_R(P)$  from PVT data. See ref 7.

Although the connection between the two characteristic material parameters, b and  $\gamma$ , is clearly very strong, inspection of the results summarized in Table I does not yield obvious correlations between b and the other material-dependent properties that are listed in the table (e.g., glass transition temperatures, characteristic hard-core volumes  $[V_{hc}]$ , or [from the LCL characterization] strength of nonbonded nearest-neighbor interactions [through  $\varepsilon$ ]). In the CFV model, b controls the sensitivity of the material to explicitly the turning temperature "knob" (beyond the extent to which  $V_{\rm free}$  changes with temperature). This can be interpreted as the effect of incremental temperature changes in altering the local motions that result in segmental relaxation. For example, consider  $\log \tau$ = -5.8 in the top panel of Figure 1; this value was picked because it is relevant to all five of the isotherms plotted. There are five values for the abscissa point  $(V_{h\sigma}/V_{free})$ , corresponding to log  $\tau$ = -5.8—hence five points on the five isotherms. But when each of those abscissa values is multiplied by the shift factor  $T^{-4.6}$ , they collapse into a single value. In general, the larger the value of b needed, the smaller the shift factor needed for such a collapse. A smaller shift factor means a lighter touch (smaller tweak) on the temperature knob is needed to compensate for the changes in free volume that are also occurring, in order to balance the two effects and put all the relaxation results on a single straight line. Quantitatively speaking, this compensation between the tuning of b and the sensitivity of  $V_{\text{free}}$  to changes in T is exactly what is reflected in the expression  $b = -(\partial \ln V_{\text{free}}/\partial \ln T)_{\tau}$ , which was introduced just before Eq. 7.

Another connection to make here is the relationship between b and the isochoric fragility,  $m_V$ . More generally, the fragility is the slope of the  $\log \tau$  versus  $T_g/T$  plot at  $T=T_g$  and characterizes the extent to which the relaxation process deviates from simple Arrhenius dependence. The common isobaric fragility,  $m_P$ , is the slope under conditions of constant P, where both T and V are changing, whereas  $m_V$  is the slope at constant V and thus isolates the changes due to T alone. For the CFV model, we have  $m_V=b\log[\tau(T_g)/\tau_{\rm ref}]$ . (The analogous relationship involving  $m_V$  and the density-scaling parameter  $\phi$  [Eq. 5] is  $m_V=\phi\log[\tau(T_g)/\tau_0]$ .) Under isochoric conditions, a larger b is associated with materials having greater isochoric fragility, which in turn, drawing from the comments above, is related to there being greater sensitivity of local activation mechanisms to small changes in temperature.

Casalini and Roland<sup>23</sup> have noted in their discussion of the density-scaling equation (here given by Eq. 5) what appears to be a rough inverse correlation between the parameters  $\gamma$  and  $\varphi$ . (See, for example, figure 2 of that work.) This suggests that the  $\varphi$  parameter serves a purpose that is similar to b, as both scale the T dependence. The inverse pattern we have shown here between  $\varphi$  and b in Figure 3 therefore has some relation to the rough inverse relationship between  $\varphi$  and  $\varphi$  found by Casalini and Roland.

One emerging trend from the results in Table I is that the nonionic small-molecule glass formers (1,1'-bis(p-methoxyphenyl)cyclohexane, 1,1'-di(4-methoxy-5-methylphenyl)cyclohexane, phenolphthalein-dimethyl-ether, orthoterphenyl) have smaller <math>b values than most of the polymeric materials, with the exception being the polysiloxanes, poly methylphenylsiloxane and poly methyltolylsiloxane. This means that small molecules show (on average) a greater relative sensitivity to free volume, compared with most of the polymers, which means that greater shifts in temperature are needed to compensate and thus collapse the isotherms into a single straight line. Another observation is that the b values across the set of polymers vary more widely—by a factor of three—for this collection of materials whose  $T_g$  range spans 170K, compared with the 65K span of  $T_g$  in the nonionic small-molecule set. This suggests that a broader range of local structural relaxation mechanisms (e.g., intermolecular as well as intramolecular backbone-related mechanisms) are involved across the variety of polymers represented, requiring quite different relaxation activation energies to be overcome. This picture is supported by the recent simulation work of Fragiadakis and Roland,  $^{40}$  which investigates the role played by intramolecular barriers (chain flexibility) in determining a system's volume sensitivity.

With regard in particular to the two newly analyzed systems, NR and PU, inspection of the b values in Table I shows that for NR, the sensitivity toward temperature versus volume puts it close to the middle of the range among polymers (intermediate b values), whereas PU has a somewhat stronger relative sensitivity toward temperature (higher b). Similar conclusions can also be drawn by inspecting  $\gamma$  or by considering the ratio of the isochoric and isobaric activation energies,  $E_V/E_P$ , where higher  $E_V/E_P$  values indicate stronger relative sensitivity to temperature. For NR, Ortiz-Serna et al. found a value of about  $E_V/E_P = 0.70$ , whereas for PU, we found  $E_V/E_P = 0.77$  (calculated using the relationship in equation 35 of ref 1, taking the ambient  $T_g$  as the reference point).

All of the work summarized involved bulk samples, but many applications of glassy materials involve thin film formulations. Very recently, we also used the CFV model to study limited relaxation data on a series of films (*T* constant, thickness varied) of poly(4-chlorostyrene) (P4CIS). We characterized the material in the bulk and used the same set of LCL parameters for the film analysis. We exploited the only available film relaxation data, which had been collected at a single temperature, to determine the one additional material parameter needed to characterize the thin-film response. In a follow-up collaborative work, newly collected experimental P4CIS relaxation data for varying film thicknesses at different temperatures showed that the CFV model predictions were extremely accurate, breaking down only for cases in which the films had become ultrathin (less than 10 nm). We therefore anticipate that the CFV model will be usefully applied to a wide range of materials for analyzing and predicting thermodynamic and dynamic behavior in both bulk and film.

### **SUMMARY**

In this article, we applied the CFV rate model to study the pressure-dependent structural dynamics in two new systems, NR and PU, and placed these new results in the context of the analysis we have completed on 11 other systems. We used the CFV model to probe the dependence of the experimental BDS  $\alpha$  relaxation time behavior as a function of temperature and (free) volume. We have shown, for example, that isotherms of  $\log \tau$  versus  $1/V_{\text{free}}$  are linear with T-dependent slopes and that this set of linear plots can be collapsed with a single parameter (b). Here, we used our full set of results on b to discuss how it characterizes the material-dependent sensitivity that each system shows toward temperature, relative to its sensitivity to (free) volume. In addition, we noted the ability of the CFV model to capture and predict dynamic behavior under sparse data conditions.

Throughout this analysis, we also made connections and comparisons with the widely applied density-scaling model for P-dependent dynamics. We demonstrated that there is an analytic relationship between the CFV b parameter and the density-scaling  $\gamma$  parameter and used the entire parameter set to show that this connection is strikingly well obeyed across a considerable range of systems, including small-molecule and polymeric rubbers and glassy melts and even an ionic liquid.

One conclusion we draw from our combined work to date is that the CFV model mechanism of local relaxation works well across the entire temperature and pressure range of practical interest. This process can be understood through a picture in which the success of segmental motion depends on overcoming an activation barrier through the combination of local free volume and sufficient thermal energy. It is worth noting explicitly that this model does not anticipate or assume a glassy "crisis" as T is lowered, only an increasing attenuation of successful segmental moves for the reasons delineated above.

We are currently working on a more detailed CFV treatment to make predictions about mobile layer thickness and relaxation times very close to an interfacial region. We anticipate that this will require only a small amount of additional thermodynamic data (surface tension as a function of

temperature) and only bulk dynamic relaxation data, with the result being that we can probe material response over length scales ranging from nanometers away from an interface, all the way in to the bulk.

# **ACKNOWLEDGEMENT**

The authors gratefully acknowledge the financial support provided by the National Science Foundation (DMR-1708542).

# **REFERENCES**

- <sup>1</sup>C. Roland, S. Hensel-Bielowka, M. Paluch, and R. Casalini, Rep. Prog. Phys. 68, 1405 (2005).
- <sup>2</sup>G. Floudas, M. Paluch, A. Grzybowski, and K. Ngai, *Molecular Dynamics of Glass-Forming Systems—Effects of Pressure*, Springer, Berlin, 2011.
- <sup>3</sup>K. Adrjanowicz, K. Kaminski, K. Koperwas, and M. Paluch, *Phys. Rev. Lett.* **115**, 265702 (2015).
- <sup>4</sup>K. Adrjanowicz, K. Kaminski, M. Tarnacka, G. Szklarz, and M. Paluch, J. Phys. Chem. Lett. 8, 696 (2017).
- <sup>5</sup>M. Tarnacka, W. K. Kipnusu, E. Kaminska, S. Pawlus, K. Kaminski, and M. Paluch, *Phys. Chem. Chem. Phys.* **18**, 23709 (2016).
- <sup>6</sup>A. Debot, R. P. White, J. E. G. Lipson, and S. Napolitano, ACS Macro Lett. **8**, 41 (2019).
- <sup>7</sup>R. P. White and J. E. G. Lipson, *Macromolecules* **51**, 7924 (2018).
- <sup>8</sup>R. P. White and J. E. G. Lipson, *J. Chem. Phys.* **147**, 184503 (2017).
- <sup>9</sup>R. P. White and J. E. G. Lipson, *Macromolecules* **51**, 4896 (2018).
- <sup>10</sup>R. P. White and J. E. G. Lipson, *ACS Macro Lett.* **6**, 529 (2017).
- <sup>11</sup>R. P. White and J. E. G. Lipson, Eur. Phys. J. E 42, 100 (2019).
- <sup>12</sup>A. K. Doolittle, J. Appl. Phys. 22, 1471 (1951).
- <sup>13</sup>M. L. Williams, R. F. Landel, and J. D. Ferry, J. Am. Chem. Soc. **77**, 3701 (1955).
- <sup>14</sup>J. D. Ferry, Viscoelastic Properties of Polymers, 2nd ed., Wiley, New York, 1970.
- <sup>15</sup>M. H. Cohen and D. Turnbull, *J. Chem. Phys.* **31**, 1164 (1959).
- <sup>16</sup>R. P. White and J. E. G. Lipson, *Macromolecules* **49**, 3987 (2016).
- <sup>17</sup>A. Grzybowski and M. Paluch, "Universality of Density Scaling," in *The Scaling of Relaxation Processes*, F. Kremer and A. Loidl, Eds., Springer International Publishing, Cham, Switzerland, 2018, pp. 77–119.
- <sup>18</sup>L. Bohling, T. S. Ingebrigtsen, A. Grzybowski, M. Paluch, J. C. Dyre, and T. B. Schroder, New J. Phys. 14, 113035 (2012).
- <sup>19</sup>J. C. Dyre, *J. Phys. Chem. B* **118**, 10007 (2014).
- <sup>20</sup>N. Gnan, T. B. Schroder, U. R. Pedersen, N. P. Bailey, and J. C. Dyre, *J. Chem. Phys.* **131**, 234504 (2009).
- <sup>21</sup>D. Fragiadakis and C. M. Roland, *J. Chem. Phys.* **134**, 044504 (2011).
- <sup>22</sup>R. Casalini, U. Mohanty, and C. M. Roland, J. Chem. Phys. 125, 014505 (2006).
- <sup>23</sup>R. Casalini and C. M. Roland, *J. Non-Cryst. Solids* **353**, 3936 (2007).
- <sup>24</sup>C. M. Roland, RUBBER CHEM. TECHNOL. **85**, 313 (2012).
- <sup>25</sup>J. E. G. Lipson and R. P. White, *J. Chem. Eng. Data* **59**, 3289 (2014).
- <sup>26</sup>R. P. White and J. E. G. Lipson, *ACS Macro Lett.* **4**, 588 (2015).
- <sup>27</sup>G. Adam and J. H. Gibbs, J. Chem. Phys. 43, 139 (1965).
- <sup>28</sup>W. Hoover and M. Ross, *Contemp. Phys.* **12**, 339 (1971).
- <sup>29</sup>Y. Hiwatari, H. Matsuda, T. Ogawa, N. Ogita, and A. Ueda, *Prog. Theor. Phys.* **52**, 1105 (1974).
- <sup>30</sup>U. R. Pedersen, N. P. Bailey, T. B. Schroder, and J. C. Dyre, *Phys. Rev. Lett.* **100**, 015701 (2008).
- <sup>31</sup>U. R. Pedersen, T. B. Schroder, and J. C. Dyre, *Phys. Rev. Lett.* **105**, 157801 (2010).

- <sup>32</sup>D. Coslovich and C. M. Roland, J. Chem. Phys. 131, 151103 (2009).
- <sup>33</sup>D. Coslovich and C. M. Roland, J. Phys. Chem. B 112, 1329 (2008).
- <sup>34</sup>D. Coslovich and C. M. Roland, J. Chem. Phys. **130**, 014508 (2009).
- <sup>35</sup>I. Avramov, J. Non-Cryst. Solids **262**, 258 (2000).
- <sup>36</sup>P. Ortiz-Serna, R. Diaz-Calleja, M. J. Sanchis, G. Floudas, R. C. Nunes, A. F. Martins, and L. L. Visconte, *Macromolecules* **43**, 5094 (2010).
- <sup>37</sup>C. M. Roland and R. Casalini, *Polymer* **48**, 5747 (2007).
- <sup>38</sup>N. Iqbal, M. Tripathi, S. Parthasarathy, D. Kumarb, and P. K. Roy, RSC Adv. 6, 109706 (2016).
- <sup>39</sup>D. Fragiadakis, R. Casalini, R. B. Bogoslovov, C. G. Robertson, and C. M. Roland, *Macromolecules* 44, 1149 (2011).
- <sup>40</sup>D. Fragiadakis and C. M. Roland, J. Phys. Chem. B 123, 5930 (2019).
- <sup>41</sup>R. Casalini, C. M. Roland, and S. Capaccioli, J. Chem. Phys. **126**, 184903 (2007).
- <sup>42</sup>C. M. Roland, K. J. McGrath, and R. Casalini, J. Non-Cryst. Solids 352, 4910 (2006).
- <sup>43</sup>W. Heinrich and B. Stoll, *Colloid Polym. Sci.* **263**, 873 (1985).
- <sup>44</sup>C. Roland and R. Casalini, *Macromolecules* **36**, 1361 (2003).
- <sup>45</sup>P. Zoller and D. Walsh, Standard Pressure-Volume-Temperature Data for Polymers, Technomic Pub Co., Lancaster, PA, 1995.
- <sup>46</sup>R. Casalini and C. Roland, *J. Chem. Phys.* **119**, 4052 (2003).
- <sup>47</sup>T. Ougizawa, G. T. Dee, and D. J. Walsh, *Macromolecules* **24**, 3834 (1991).
- <sup>48</sup>M. Paluch, C. Roland, and S. Pawlus, J. Chem. Phys. **116**, 10932 (2002).
- <sup>49</sup>M. Paluch, R. Casalini, A. Patkowski, T. Pakula, and C. Roland, *Phys. Rev. E* 68, 031802 (2003).
- <sup>50</sup>M. Paluch, S. Pawlus, and C. Roland, *Macromolecules* **35**, 7338 (2002).
- <sup>51</sup>P. Panagos and G. Floudas, *J. Non-Cryst. Solids* **407**, 184 (2015).
- <sup>52</sup>A. Panagopoulou and S. Napolitano, *Phys. Rev. Lett.* **119**, 097801 (2017).
- <sup>53</sup>S. Hensel-Bielowka, J. Ziolo, M. Paluch, and C. Roland, J. Chem. Phys. 117, 2317 (2002).
- <sup>54</sup>M. Paluch, C. Roland, R. Casalini, G. Meier, and A. Patkowski, J. Chem. Phys. 118, 4578 (2003).
- <sup>55</sup>R. Casalini, M. Paluch, and C. Roland, *Phys. Rev. E* **67**, 031505 (2003).
- <sup>56</sup>R. Casalini, M. Paluch, and C.M. Roland, J. Phys.-Condens. Matter 15, S859 (2003).
- <sup>57</sup>M. Paluch, R. Casalini, A. Best, and A. Patkowski, *J. Chem. Phys.* **117**, 7624 (2002).
- <sup>58</sup>M. Naoki, H. Endou, and K. Matsumoto, *J. Phys. Chem.* **91**, 4169 (1987).
- <sup>59</sup>M. Naoki and S. Koeda, *J. Phys. Chem.* **93**, 948 (1989).
- <sup>60</sup>A. Rivera-Calzada, K. Kaminski, C. Leon, and M. Much, *J. Phys. Chem. B* **112**, 3110 (2008).
- <sup>61</sup>M. Paluch, S. Haracz, A. Grzybowski, M. Mierzwa, J. Pionteck, A. Rivera-Calzada, and C. Leon, *J. Phys. Chem. Lett.* 1, 987 (2010).

[Received July 2019, Revised October 2019]